THE STRUCTURE OF THE UPPER ATMOSPHERE

M. Nicolet

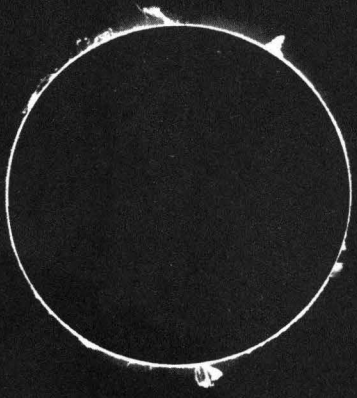

Reprinted from

RESEARCH IN GEOPHYSICS

Volume 1: Sun, Upper Atmosphere, and Space

Copyright © 1964 by
The Massachusetts Institute of Technology

CHAPTER 10

THE STRUCTURE OF THE UPPER ATMOSPHERE

M. Nicolet

1. Introduction

Before the International Geophysical Year our knowledge of the upper atmosphere was based on the interpretation of spectroscopic and radio-electric observations made at ground level and on a few rocket results obtained in the United States. Spectroscopic analysis of the night airglow has led to the detection of radiation emitted by atomic oxygen, molecular oxygen, and the OH radical. No emission from the molecular spectrum of nitrogen has been identified. Twilight spectrum results have also been useful. They have shown that N_2^+ bands and OI red line are present up to very high altitude. On the other hand, the general conclusion obtained from studies of the twilight and night airglow was that most excitation processes were due to chemical reactions occurring below 100 km. Auroral spectra exhibit lines and bands of molecular nitrogen which do not occur in the normal airglow spectrum. The spectral behavior of an aurora, including the displaced lines of atomic hydrogen, were conclusive evidence that charged particles are responsible for auroral displays. Some information concerning atmospheric composition was also gained through auroral analysis since the presence of N_2^+ bands in sunlit auroras up to 1000 km clearly indicates the presence of molecular nitrogen at high altitudes. The deduction of an absolute composition of the atmosphere from spectroscopic studies is difficult because of the different excitation processes involved.

Determinations of electron density profiles have often been misleading due to the fact that the actual heights of the ionization peaks were not given. For example, the conception of a maximum of photoionization above 200 km associated with the F_1-peak has led, during the past several years, to a misinterpretation of the atmospheric parameters involved in the analysis of the atmospheric structure.

A major advance in aeronomy occurred when the U.S. Naval Research Laboratory began using rockets for such work. At the end of 1953 [6] when the International Geophysical Year was planned, the ultraviolet solar spectrum was known down to about 2000 Å, and the daytime distribution of ozone had been observed up to 70 km and deduced theoretically up to 90 km. The vertical distribution of molecular oxygen was experimentally and theoretically deduced as being not in photochemical equilibrium but rather almost in diffusive equilibrium. The X-ray solar radiation was detected as being important in the range of 20–60 Å while Lyman α was first detected at altitudes below 75 km. Various pressure measurements were made below 100 km, but only three rocket flights above that height gave densities at 160 km and 200 km. Few rocket observations have been made between 100 and 200 km and the pressure at 100 km is not well known. Adopting a pressure of $(2.5 \pm 1.0) \times 10^{-4}$ mm Hg at 100 km, it is not yet possible to determine the exact range of the real variations. All upper atmospheric models are based on boundary conditions near the 100-km level; hence, any analysis of the upper atmosphere structure is subject to an uncertainty due to the unknown variations of the pressure in the lower thermosphere.

The lack of density observations made by rockets has been compensated for by the large number of satellite launchings which began with the first Sputnik at the beginning of the IGY. The Explorer and Vanguard satellites have made possible the study of the density variation over a height range of more than 500 km. The vertical distribution of thermospheric densities is now interpreted up to the atomic hydrogen belt, with a scale height which continually increases with height. Before attempting to draw a diagram of the neutral atmosphere, it is necessary to emphasize the terminology which was introduced by S. Chapman and which is now adopted by the International Union of Geodesy and Geophysics and the World Meteorological Organization. The vertical distribution of the temperature is the basis of such a nomenclature. Starting from the definition used in meteorology that the lowest atmospheric region is the troposphere heated by the earth's surface and its upper boundary the tropopause where the temperature gradient changes, it is possible to define regions representing alternately negative and positive gradients of the temperature. In this system the stratosphere extends up to a temperature peak in the neighborhood of 50 km where the upper atmosphere studied by physicists and radio engineers begins.

Thus, the atmosphere can be described as follows:

Earth's surface:	Temperature, 273°K ± 20°K.
Troposphere:	Temperature decreases with height.
Tropopause:	Temperature minimum, 210°K ± 20°K, and altitude 13 ± 5 km.

Stratosphere:	Temperature increases with height.
Stratopause:	Temperature maximum, 273°K ± 20°K, and altitude 50 ± 5 km.
Mesosphere:	Temperature decreases with height.
Mesopause:	Temperature minimum, 190°K ± 25°K, and altitude 85 ± 5 km.
Thermosphere:	Temperature increases.
Thermopause:	Beginning of an isothermal region.

The thermosphere temperature and its gradient vary with latitude and season. The variation with time of day and solar activity is remarkable.

The vertical distribution of the temperature depends on the local heat source and is related to the process of heat transport. In the troposphere, the heat source is the earth's surface and convection is the principal process of heat transport. Absorption of solar ultraviolet radiation by ozone and emission of infrared radiation in the stratosphere show that the heat budget involves radiative processes. The mesosphere, in which absorption processes are unimportant compared to heat loss processes, is a relatively unstable region.

Above the mesopause all ultraviolet radiation of wavelength shorter than 1750 Å is gradually absorbed and a fraction of the absorbed energy is used for the heating of the thermosphere. Atomic oxygen can radiate in the infrared at about 63 μ but convection in the lower thermosphere and conduction in the upper thermosphere are the principal processes of heat transport.

Composition must be introduced in the atmospheric nomenclature, for it is necessary to consider two essential divisions: the homosphere in which the composition is uniform despite the presence of minor constituent layers (i.e., ozone), and the heterosphere in which the mean molecular mass varies because such physical processes as molecular dissociation or diffusion of gases alter the composition.

Chapman's terminology is clear and satisfactory. It involves temperature, mean molecular mass, and composition, i.e., all the parameters necessary for defining an atmosphere for which hydrostatic conditions can be used. However, above the thermopause in the *isothermal region*, the mean free path of neutral atoms becomes so large that the hydrostatic law becomes inapplicable. The exosphere begins at a certain altitude called the *critical level*. This is where neutral atoms describe various orbits in the gravitational field of the planet.

Since the earth's atmosphere under static equilibrium is considered as a perfect gas composed of molecules and atoms of which only a small fraction is represented by charged particles, the *ionosphere* includes all atmospheric regions in which the behavior of ions and electrons influenced by the earth's magnetic field is studied. However, above a certain altitude,

charged particles are governed primarily by the earth's magnetic field rather than its gravitational field. This outermost region of a planetary atmosphere is called the *magnetosphere*. Its outer boundaries reach out into interplanetary space.

2. The Chemosphere

Nighttime airglow observations [42] made by rockets show that the principal radiations, namely from OI (λ 5577 Å), Na (λ 5892 Å), O_2 bands, and hydroxyl bands, occur at relatively low height with emission peaks below 100 km. The aeronomic processes involved in producing such radiation correspond to chemical processes and cannot be associated with ionospheric processes. The nightglow cannot be caused by particles entering the atmosphere down to 100 km. However, photoelectrons can lead to appreciable airglow emission during the daytime in the ionospheric regions where the electron production is important.

Since Chapman drew attention to the chemical reservoir for the production of the airglow, the basic theories have considered the behavior of atomic oxygen in the mesosphere and lower thermosphere. Photochemical processes in the mesosphere and lower thermosphere are controlled by solar radiation for $\lambda > 1700$ Å. This leads to an atomic oxygen concentration not less than the ozone concentration for daytime conditions [3] at the stratopause. Ozone and oxygen atoms are important constituents in the mesosphere and they cause the introduction of many other chemical processes. A great variety of collision reactions are possible in an oxygen atmosphere (O_2, O, O_3) bathed in ultraviolet radiation and containing minor constituents such as water vapor, methane, and nitrogen oxides.

Free oxygen atoms are subject to reactions such as

$$O_2 + O + M \rightarrow O_3 + M \tag{1}$$

and

$$O_3 + O \rightarrow 2O_2 \tag{2}$$

During the night, atomic oxygen disappears through the rapid formation of ozone in the lower part of the mesosphere where the number of three-body collisions is very large. At the mesopause level, the ozone concentration grows at a smaller rate and the recombination of oxygen atoms by the process

$$O + O + M \rightarrow O_2 + M \tag{3}$$

is always small.

Methane is subject to direct photodissociation by Lyman α in the upper mesosphere. Methane disappears also by the oxidation process [2]

$$CH_4 + O \rightarrow CH_2 + H_2O \tag{4}$$

The presence of water vapor in the mesosphere is therefore not related to an upward transport from the stratosphere but to its production in the stratosphere itself. The photodissociation of H_2O leads to the production of hydrogen atoms. A hydrogen-oxygen atmosphere is very complicated since many important reactions can exist. A single free or combined hydrogen atom reacts with one of the allotropic forms of oxygen as

$$H + O_2 + M \rightarrow HO_2 + M \tag{5}$$

$$H + O_3 \rightarrow OH + O_2 \tag{6}$$

$$OH + O \rightarrow H + O_2 \tag{7}$$

$$HO_2 + O \rightarrow OH + O_2 \tag{8}$$

Other reactions such as

$$OH + OH \rightarrow H_2O + O \tag{9}$$

$$HO_2 + HO_2 \rightarrow H_2O_2 + O_2 \tag{10}$$

$$OH + HO_2 \rightarrow H_2O + O_2 \tag{11}$$

are also important processes. In the lower thermosphere, equilibrium conditions can be found for H, OH, and HO_2. The elements H_2O and H_2 should follow a vertical distribution subject to a departure from photochemical equilibrium conditions in the entire mesosphere. Since the rate of oxidizing reactions falls off rapidly with altitude, hydrogen compounds become less important with height and the element is left in atomic form in the lower thermosphere. Free hydrogen atoms diffuse in the mixing region and the rate of the upward flow controls the escape flow in the exosphere. On the other hand, H_2O is produced at the bottom of the mesosphere and this is an important source of water vapor in the middle atmosphere. (The dissociation of methane is also a source of carbon dioxide which must be subject to a downward transport.)

The production of nitric oxide is related to the production of nitrogen atoms [2, 40] by direct processes such as the predissociation of N_2 or by dissociative recombination of NO^+, an ion produced by reactions like

$$O^+ + N_2 \rightarrow NO^+ + N \tag{12}$$

$$O_2^+ + N_2 \rightarrow NO^+ + NO \tag{13}$$

Two important reactions can be considered as the loss processes of atomic nitrogen, which is a minor atmospheric constituent:

$$N + O_2 \rightarrow NO + O \tag{14}$$

and

$$N + NO \rightarrow N_2 + O \tag{15}$$

Reaction 13 should play a role in the *D*-region while reaction 12 occurs in the *F*-region. As far as nitric oxide is concerned, reactions 14 and 15 control its concentration. At sufficiently low levels, i.e., in the mesosphere, nitric

oxide has a very long lifetime. Any NO molecule going downward at mesopause will have the tendency to follow a mixing distribution in the mesosphere. At sufficiently low levels, NO_2 must be considered, keeping in mind such reactions as:

$$NO_2 + O \rightarrow NO + O_2 \tag{16}$$

$$NO + O_3 \rightarrow NO_2 + O_2 \tag{17}$$

$$NO + O \rightarrow NO_2 \tag{18}$$

and

$$NO_2 + h\nu \rightarrow NO + O \tag{19}$$

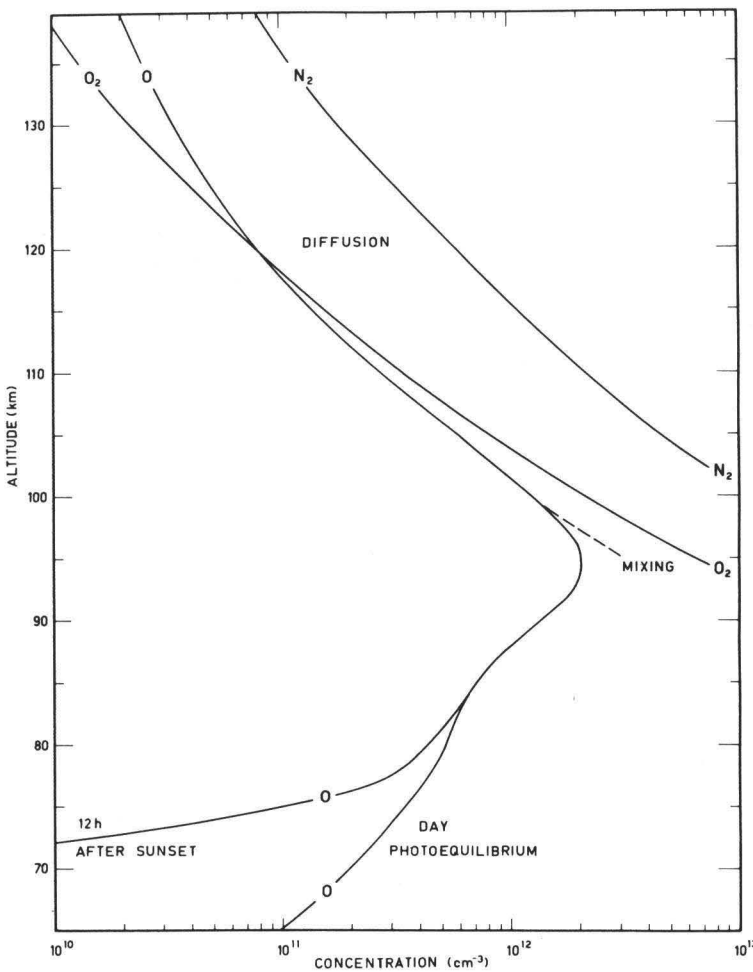

FIG. 1. The vertical distribution of oxygen and nitrogen in the upper mesosphere and lower thermosphere. The absolute values have been determined by assuming a pressure of 3×10^{-4} mm Hg at 100 km. A variation of the pressure at that level may be considered as a variation of the reference height; for example, 100 km ± 5 km.

Evidence supporting several of the preceding deductions can be found through the interpretation of the airglow spectrum and of the ionic constitution of the upper atmosphere.

The fundamental problem of the chemosphere starts from the dissociation of molecular oxygen. This dissociation depends mostly on the absorption of solar radiation of wavelengths less than 1750 Å and corresponds to a rate coefficient of about 5×10^{-6}/sec at zeroth optical depth. In the lower thermosphere with finite optical depth, the dissociation times become very long and diffusion leads to a departure from photochemical conditions. Figure 1 is intended to illustrate the conditions under which the problem of oxygen dissociation must be considered.

It is convenient to consider that the heterosphere, i.e., the atmospheric region where the mean molecular mass decreases with height, begins above the mesopause due to the partial dissociation of oxygen. The structure of this region is still very uncertain (recall the uncertainty in the pressure at 100 km). Therefore, it is necessary to select a reference level for diffusion. We have chosen 120 km as this level because it is almost certain that all the principal constituents are in diffusion equilibrium for steady-state conditions. Also, the introduction of a temperature gradient which increases rapidly can be made because the kinetic energy of a vertical column in this region is of the same order as the total solar ultraviolet energy absorbed in one day.

Thus, the thermosphere can be characterized with order in height by the dissociation of oxygen, the diffusion of all constituents, and the rapid increase in temperature.

3. Density in the Heterosphere

The heterosphere has been studied very extensively since the IGY [5, 32] and much detailed information is available from satellite data. Density determinations have been made by various authors following the initial calculations of the acceleration of the first two satellites (1957α and β, Sputniks I and II) whose perigees were below 225 km. The satellites Vanguard I (1958 β_2), Explorer I (1958 α), Explorer IV (1958 ϵ), and Sputnik III (1958 δ) have made an analysis of the densities possible at altitudes of approximately 650 km, 350 km, 260 km, and 220 km corresponding to the perigees of the above satellites. A synthesis of the results obtained through August, 1958 is given in the Volume XII of the Annals of the IGY [32]. The first Sputnik was launched during the period of maximum solar activity in October, 1957 when the thermopause temperature was a minimum of 2000°K for daytime conditions and greater than 1500°K for nighttime conditions. An approximate value of the density near 230 km is estimated to be 2×10^{-13}, which leads to about 4×10^{-13} gm/cm^3 at 200 km. Exclusive of systematic errors introduced in the deter-

mination of the absolute values of the density, various spurious effects [24] were noticed, such as variations of density with latitude which are due to the effect of the earth's equatorial bulge. This effect is only of the order of 5 per cent for Vanguard I, but has reached 40 per cent for Sputnik III. Several previous analyses should be modified to take into account the latitude variation of perigee. A consistent picture of the vertical distribution of air density cannot be obtained if the exact heights above sea level are not used. "Wiggles" or "kinks" in density curves below 300 km have been interpreted as due to peaks in the temperature. Comparison of the results obtained by several authors [52] (King-Hele, Paetzold, Priester and Martin [49]) shows that the method of analysis is involved in these deductions since the peaks do not occur at the same height for the same satellites. For example, a maximum and a minimum of temperature has been deduced near 220 km. Therefore, the available atmospheric density data near 200 km are not yet precise enough to determine the absolute density value and its real variations. Variations of ± 15 per cent cannot be necessarily considered as real modifications of atmospheric conditions, and they can lead to wrong deductions of atmospheric parameters.

A study of the observations from 300 km to 700 km, i.e., over a large range of altitudes, leads to the conclusion that the temperature variation is *not* the only important parameter determining the vertical distribution but that the variation of the mean molecular mass is also a controlling factor. The variation of ρ, the mass-density, which is expressed by

$$\frac{d\rho g}{\rho g} = -\frac{1+\beta}{\beta}\frac{dH}{H} \tag{20}$$

(where $\beta = dH/dr$ is the gradient of the atmospheric scale height H, and g is the gravitational acceleration) indicates that up to the maximum perigee height of Echo I ($\sim$1600 km) the major varying parameter is the mean molecular mass.

Studies of the fluctuations in the accelerations of satellites Vanguard I and Sputnik III, which were found to be in phase by Jacchia [16], showed that this atmospheric variation was correlated with solar radiation (Priester [48]). Furthermore, Jacchia [15] detected another effect. This led to a correlation between the increase of satellite drag and geomagnetic disturbances. Finally, the difference in density between daytime and nighttime conditions was recognized (Jacchia [18]), with a strong diurnal effect at highest altitudes. A diurnal effect can only be explained if the temperature of the isothermal region varies considerably between night and day. Furthermore, the normal heating of the upper atmosphere takes place by electromagnetic radiation and any hypothesis introducing a direct or indirect effect of particle cannot be taken too seriously, excepting auroras. The good correlation between radio-solar fluxes and atmospheric

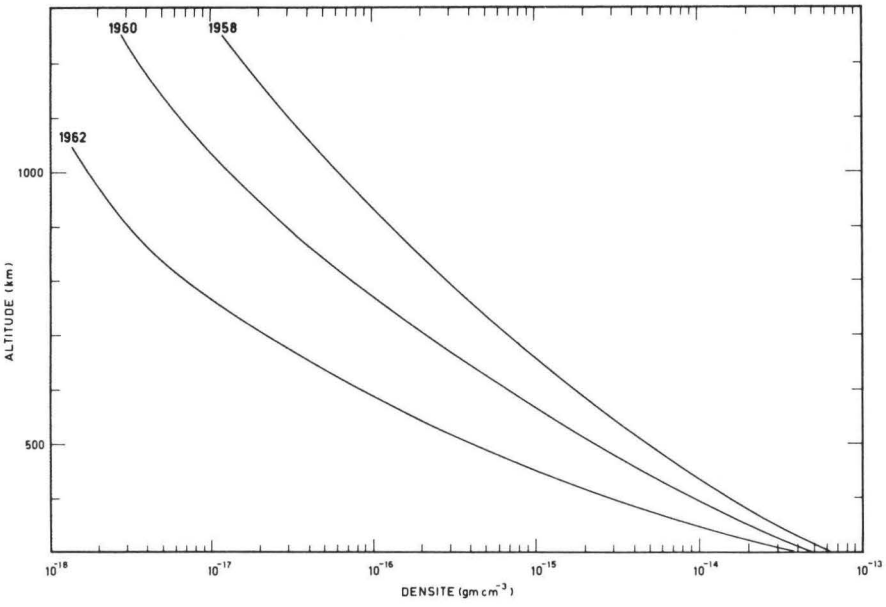

FIG. 2. Average density values for decreasing solar activity from 1958 to 1962. The density variation above 300 km is essentially associated with the temperature variation of the isothermal region.

densities [47] also shows that ultraviolet radiation is responsible for atmospheric heating. Solar activity was at its maximum when the first satellite was launched. Since then there has been a continuous decrease, almost reaching a minimum in August, 1962. Figure 2 illustrates average conditions for 1958, 1960, and 1962, and indicates the large density variation due to the decrease of the ultraviolet heating of the thermosphere during this period.

4. Variation of Solar Activity and Temperature

The solar radio flux is composed of a basic component corresponding to the general emission of the solar disc and of a slowly varying component associated with sunspots. There is a way in which radio observations can be used as indices of solar activity. A choice of radiations in the range of 1000 to 10,000 Mc/sec is justified because they are emitted from that part of the solar atmosphere where the majority of ultraviolet emissions are produced. Furthermore, there is a correlation between the Zurich sunspot number and a particular radio flux when average values are taken over a sufficiently long period [38] such as a 27-day or monthly period. A plot (Fig. 3) of the Wolf number $\bar{R}_{27}$ with the radio flux $\bar{S}_{27}$ (10.7 cm) shows where a linear relationship is valid. It should be noticed that variations of

±10 per cent are significant for average values. Daily values have variations greater than ±20 per cent and are unsuitable as a solar index. Differences between the fluxes emitted from 1000 Mc/sec to 10,000 Mc/sec which occur with variations of solar activity exclude any peculiar behavior at a specific frequency [37]. Certain "effects" can apparently be attributed to drifts of instrumental origin.

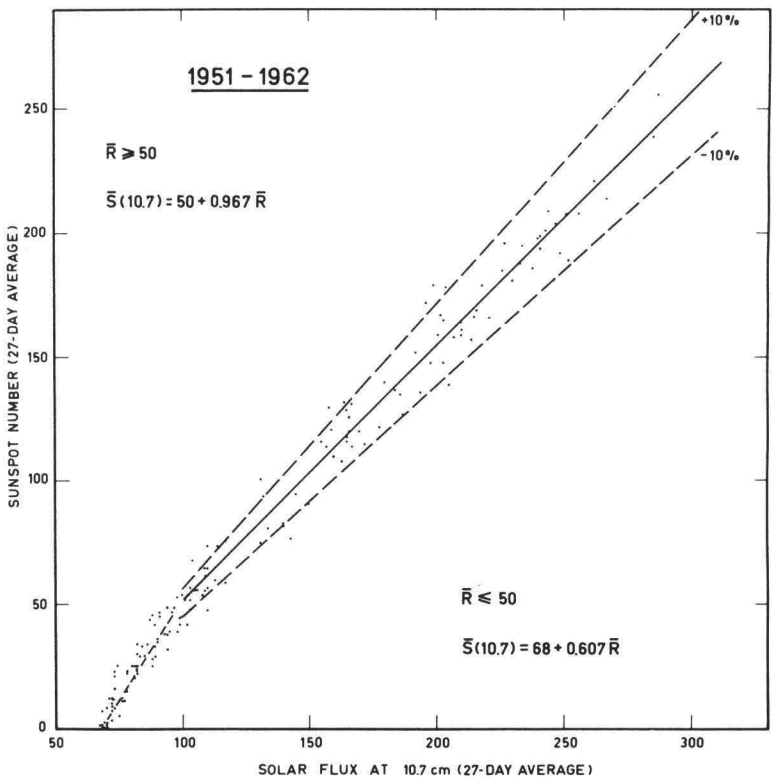

FIG. 3. The relationship between the relative sunspot number and the radio flux at 10.7 cm. A linear relationship cannot be used for the entire solar cycle. From M. Nicolet [38].

A complete analysis shows that the ratio of two solar radio fluxes does not remain constant during an entire solar cycle. A typical example is the flux variation for two wavelengths such as 8 cm and 10.7 cm. Figure 4 shows the gradual difference in the ratio of 27-day mean values. Both fluxes are identical near 200 units while the ratio is reversed for lower and higher values of solar fluxes. The ratios of the maximum 27-day mean value reached in October–December, 1957 and of the minimum 27-day mean value reached in May, 1954 are 3.7 and 4.2 for 8 cm and 10.7 cm, respec-

tively. The same ratios become 1.6 and 4.5 at 3.2 cm and 30 cm, respectively.

The ratios of the minimum daily fluxes during the maximum sunspot of 1957 and of the minima 27-day mean values increase with the wavelength. The ratios are 1.2, 2.2, 2.5, 2.8, and 3.0 for 3.2 cm, 8 cm, 10.7 cm, 15 cm, and 30 cm, respectively. A variation from 1.2 to 3.0 shows that it is difficult to determine the amplitude of the quiet-sun variation as related to the

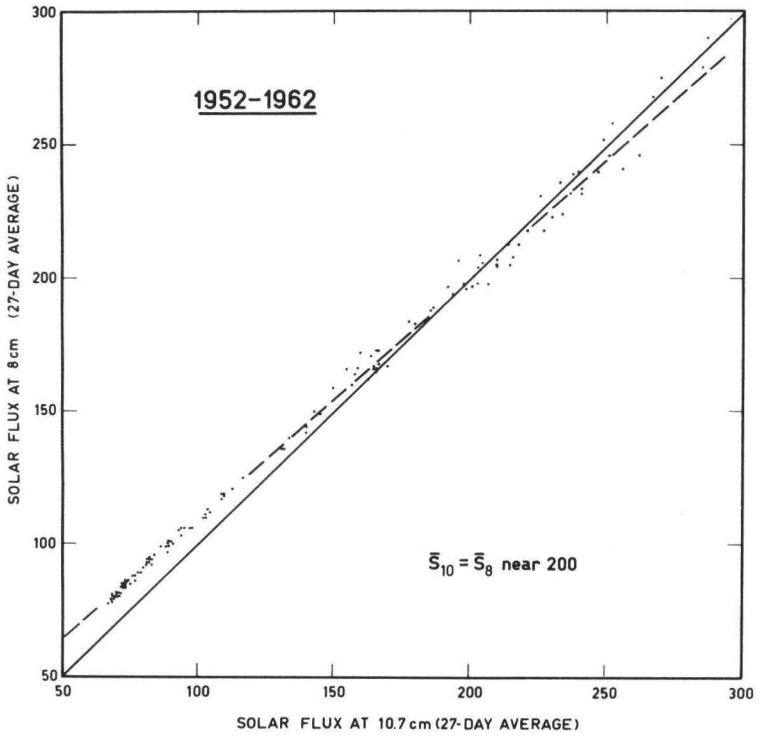

FIG. 4. The relationship between radio fluxes at 8 cm and 10 cm from minimum to maximum solar activity. It shows that the ratio of these fluxes varies with solar activity. From Nicolet [38].

ultraviolet flux. When 27-day mean fluxes are compared over a whole solar cycle (Fig. 5), one finds a departure from a smooth curve. Individual ratios are affected by about ± 5 per cent, which corresponds to errors accepted for *good* measurements of the solar radio fluxes.

Finally, the maximum variation which is observed in the solar radio flux from 1000 Mc/sec to 10,000 Mc/sec, i.e., the ratio of the maximum daily flux reached in 1957 and the minimum daily flux reached in 1954 is less than 6. It is less than the change in the X-ray flux absorbed in the ionospheric E-layer, which is 7 for a solar cycle [10]. The behavior of the

solar radio flux is not a good representation of the solar X-ray flux, but a specific frequency can represent, approximately, the major part of the ultraviolet flux associated with atmospheric heating.

Above a certain altitude, i.e., at the thermopause, the increase of atmospheric scale height with altitude is due to the decrease of the mean molecular mass in an isothermal atmosphere. The variation of thermopause temperature is related to the variation of the ultraviolet heating and conduction cooling. There is a relationship between solar radio flux and thermopause temperature. Jacchia [17], using Nicolet's atmospheric model [39], introduced a linear relationship between the solar flux at 10

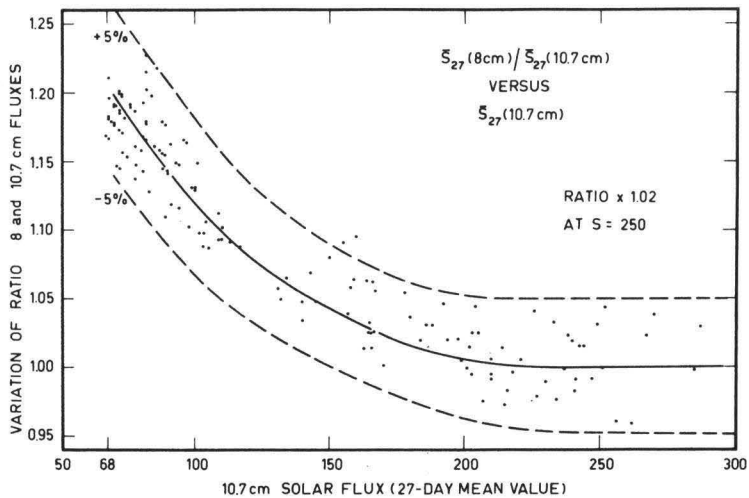

FIG. 5. The ratio of radio fluxes at 8 cm and 10.7 cm from minimum to maximum values of the solar flux. A variation of ±5 per cent for individual ratios being an indication of errors in the temperature determination. From Nicolet [38].

cm and the thermopause temperature. This was adopted also by Harris and Priester [12] and Paetzold [43].

In light of the preceding discussions the form of such an equation for the thermopause temperature may be written as follows:

$$T = T_0 + a\bar{S}_{27} + b\,\Delta S \tag{21}$$

where $\bar{S}_{27}$ is the mean value for a 27-day period and ΔS represents the oscillation during such a period. T_0, a, and b are constants which are obtained from observational analysis. For average nighttime conditions, we write

$$\bar{T}_{\text{night}} = 280°\text{K} + (4°.6 \pm 0.25)\,\bar{S}_{27}(8\text{ cm}) \tag{22}$$

in which a variation of ±5 per cent for any average absolute value of the

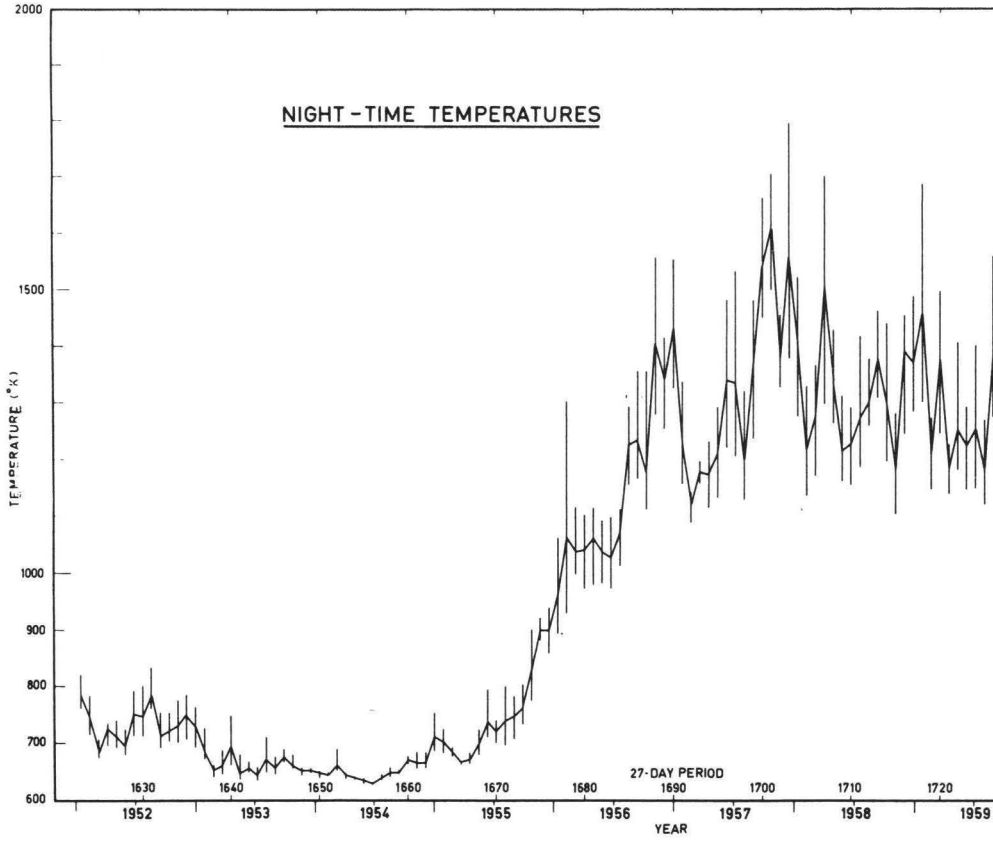

FIG. 6. Average nighttime temperatures (27-day mean values) at the thermopause level and the from 1952 to 1962. Magnetic storm effects are not included. From Nic

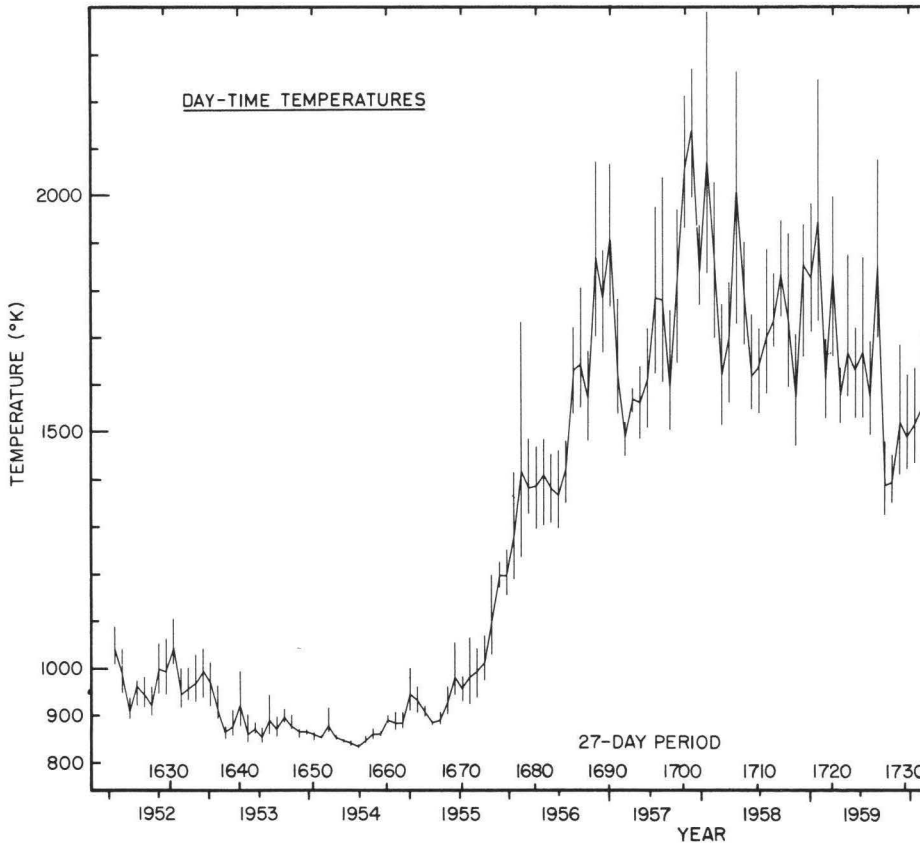

FIG. 7. Average daytime temperatures (27-day mean values) at the thermopause level and the 2
from 1952 to 1962. Magnetic storm effects are not included. From Nic

solar flux is taken into account by the term $\pm 0.25S$. This fluctuation indicates an uncertainty of $\pm 50°$K for a solar radio flux of 200 units.

The study of the 27-day oscillation made by Jacchia and Slowey [19] can be expressed by

$$T = \bar{T} + (2°.5 \pm 0.25)\, \Delta S(8 \text{ cm}) \tag{23}$$

in which a variation of ± 10 per cent takes into account differences which often occur in the daily fluxes.

The nighttime temperature is given by combining Equations 22 and 23 as

$$T_{\text{night}} = 280°\text{K} + (2°.1 \pm 0.25)\, \bar{S}_{27} + (2°.5 \pm 0.25)\, S \tag{24}$$

$dT/d\bar{S}_{27} = 2°.1 \pm 0.25$ is due only to the ultraviolet radiation and not the solar wind or corpuscular radiation; $dT/dS = 2°.5 \pm 0.25$ represents the contribution of the ultraviolet radiation which is due to the 27-day oscillation and it has a smaller weight then the basic component $\bar{S}_{27}$ which represents the entire solar disk.

In order to obtain the average daytime conditions we use Jacchia's relation

$$\bar{T}_{\text{day}} = 1.3\bar{T}_{\text{night}} \tag{25}$$

It is possible to illustrate the variation of daytime and nighttime temperatures over a whole solar cycle with formulas 24 and 25. Figures 6 and 7 indicate the temperatures reached during the IGY, when the solar cycle was its maximum, and the temperatures which will be observed during IQSY for a quiet-sun period.

5. Diffusion

The composition of the thermosphere is characterized by three principal constituents, namely molecular nitrogen and atomic and molecular oxygen. It is not possible, however, to explain the vertical distribution of density in the whole heterosphere without considering helium and atomic hydrogen. The helium belt, which was introduced by Nicolet [36, 35], is now accepted as explaining the neutral and ionized atmosphere above 500 km (the last objection was given by Paetzold and Zschörner [44]). A complete helium-hydrogen analysis has been made by Kockarts and Nicolet [27, 28] considering a diffusion steady state involving the thermal diffusion effect in the thermosphere. It should be pointed out here that Paetzold [43] and also Harris and Priester [12] have not included thermal diffusion in their computations and thus their atmospheric models must be modified above a certain altitude.

The hydrogen distribution which was determined by Bates and Patterson [4] and Kockarts and Nicolet [27, 28] is based on the following general

equation, applicable to a minor constituent in a steady state:

$$\frac{\partial n_1}{\partial r} + \frac{n_1}{H_1}[1 + \beta_1^*(1 + \alpha_T)] + \frac{F_a}{D_1}\left(\frac{a}{r}\right)^2 = 0 \tag{25}$$

In this equation, r is the distance to the earth's center, and $a = r$ is the lower boundary of the region under study. The scale height H_1 of the minor constituent of mass m_1 is

$$H_1 = kT/m_1 g \tag{26}$$

with a gradient

$$\beta_1 = \beta_1^* + 2H_1/r \tag{27}$$

The thermal diffusion factor is denoted by the symbol α_T. The last term of Equation 25 expresses the continuity of the flux F

$$F = n_1 w_1 = F_a(a/r)^2 \tag{28}$$

where w_1 is the diffusion rate of the minor constituent. The diffusion coefficient is introduced in the following form:

$$D_1 = \frac{3\sqrt{\pi/2}}{8\pi\sigma^2 f}\left(1 + \frac{m}{m_1}\right)^{1/2} \frac{(gH)^{1/2}}{n} \tag{29}$$

where m and H are the mean molecular mass and the scale height of the principal constituent with concentration n; $\sigma f^{1/2}$ represents the effective radius for diffusion. The diffusion flux F_{DM} for mixing conditions is

$$F_{DM} = \frac{n_1}{n}\frac{g}{T^{1/2}}\frac{3\sqrt{\pi/2}}{8\pi\sigma^2 f}\left(1 + \frac{m}{m_1}\right)^{1/2}\left(\frac{m}{k}\right)^{1/2}\left(1 - \frac{m_1}{m} - \beta^*\alpha_T\right) \tag{30}$$

where β^* is defined by a formula like Equation 27 in which H is the atmospheric scale height. For any minor constituent the diffusion flux in mixing conditions depends on the constant ratio n_1/n, is proportional to the product $(a^2/r^2)\,T^{-1/2}$, and is related to the height variation of $\beta^*\alpha_T$. Thus, the escape flux of a minor constituent of small mass m_1 is controlled by diffusion conditions in the mixing region. The escape flux F_c at the critical level r_c is given by

$$F_c = n_c v_E \tag{31}$$

in which v_E denotes the effusion velocity. This velocity depends essentially on the temperature since it is proportional to the exponential factor $[-r_c m_1 g/kT]$. The escape flux for a steady state obtained from Equations 30 and 31 is given by the following expression:

$$a^2 F_{DM} = r_c^2 F_c = n_c r^2 v_E \tag{32}$$

Thus, the concentration n_c depends on the diffusion flux in the mixing region.

The last term of Equation 25 is practically negligible for helium and diffusion equilibrium can be applied to a constituent for a constituent of mass $m_1 \geq 4$. In the thermosphere, Equation 32 must be used for atomic

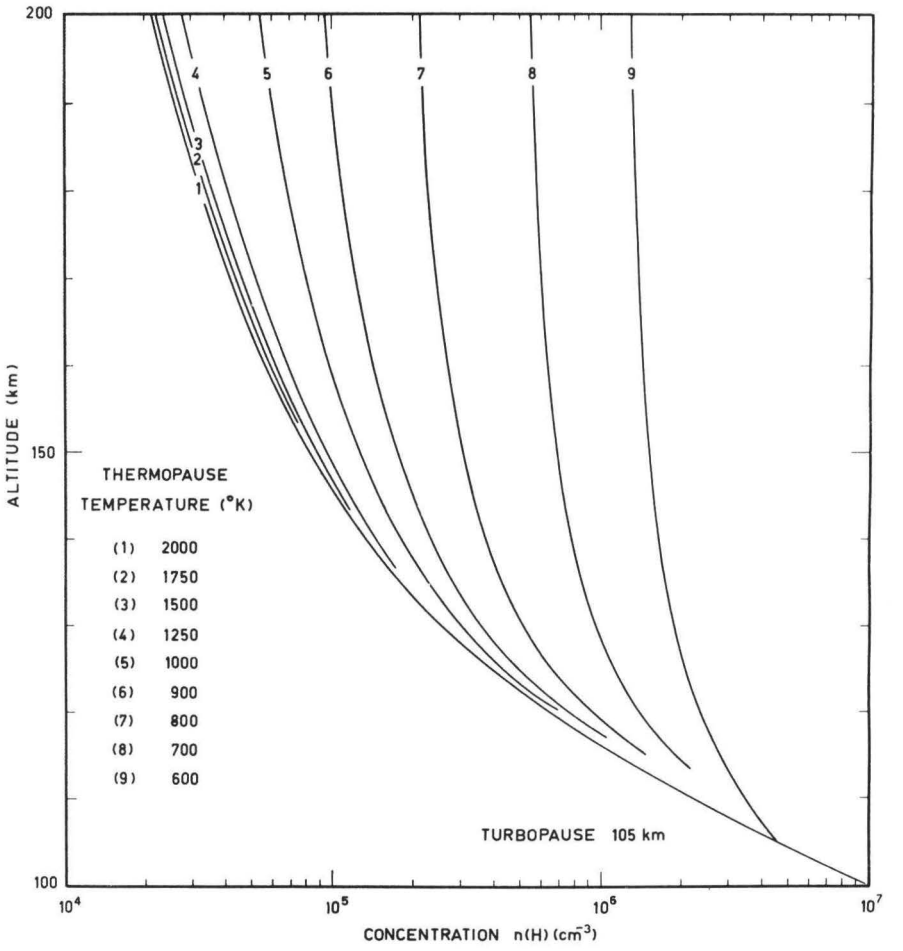

FIG. 8. The vertical distribution of atomic hydrogen between 100 km and 200 km for various thermopause temperatures. At high solar activity (thermopause temperature $T > 1250$°K), very small variation of the density with temperature. At low solar activity ($T < 1250$°K) density variations of an order of magnitude at 200 km. From Kockarts and Nicolet [28].

hydrogen. An illustration of the vertical distribution of atomic hydrogen is presented in Figure 8. The concentration n(H) at 200 km is seen to depend on the thermopause temperature. Variation of temperature from 2000–1000°K leads to an increase of only a factor of 2 in the concentration

at 200 km, the variation of temperature from 1000–700°K corresponds to an increase of a factor 10 for the concentration.

Diffusion is very important in the entire heterosphere. In order to illustrate how strongly the lightest constituents can be affected, Figure 9 shows the variation with temperature of concentration of H, He, and O above 1000 km. Helium is the principal constituent for temperatures greater than 1000°K, and at the lowest temperatures (minimum solar activity)

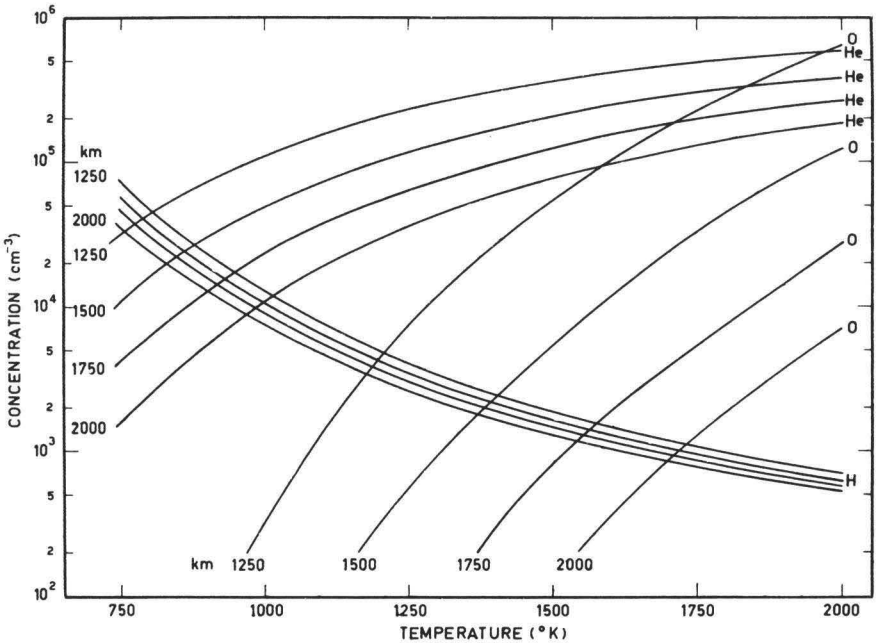

FIG. 9. The variation of H, He, and O concentrations above 1000 km with thermopause temperature. There is a rapid decrease of atomic oxygen and a small decrease of helium while atomic hydrogen increases with decreasing temperature. From Kockarts and Nicolet [28].

atomic hydrogen reaches a concentration about 100 times greater than during maximum solar activity.

6. Thermobalance in the Heterosphere

Diffusion in the heterosphere implies that conduction is also important. It is a normal consequence of the high temperature gradients in the thermosphere. Spitzer [51] has drawn attention to the effect of thermal conductivity as compared with the heating due to absorbed solar radiation. Bates [2] analyzed the thermobalance by considering the energy gained

by absorption of ultraviolet absorption and lost through radiation and conduction. Johnson [20] has shown that the temperature cannot increase above a certain height if solar electromagnetic radiation is the sole predominant source. Nicolet [37] demonstrated that all atmospheric models based on an increasing gradient of temperature with height were not acceptable and that the normal tendency for daytime or nighttime conditions is to attain isothermy above a variable height level called the thermopause, even for diurnal temperature variations reaching 500°K.

The flux density of heat,

$$E = -AT^{2/3} \operatorname{grad} T \tag{33}$$

(A is a numerical factor depending on the atmospheric constitution), can be introduced in the continuity equation:

$$\rho c_v \frac{\partial T}{\partial t} + \operatorname{div} E = P - L \tag{34}$$

where c_v is the specific heat at constant volume with density ρ, and L denotes the radiative loss of heat per unit of time and volume. In the terrestrial atmosphere this loss is due only to Bates' process of emission from atomic oxygen at 63μ. The production of heat P cannot be defined with great precision. If it is taken as directly proportional to the ionizing radiation, conclusions are obtained which are not acceptable for a problem of thermobalance in the heterosphere. For example, Harris and Priester [12] have introduced, in addition to the ultraviolet heating, a peculiar heating of the same amount which according to them derives its energy from solar corpuscular radiation and/or the solar wind. In fact, the vertical distribution of an ultraviolet heat source cannot be simply related to the ionizing fluxes which depend on the solar zenith distances. Various processes such as ionization and excitation are simultaneously involved with chemical reactions so that there is a certain redistribution of the heat source by conduction before the complete transformation of ultraviolet radiations into heating occurs. Even for nighttime conditions an internal heat source cannot be avoided since there are recombination processes. The solution of the time-dependent heat conduction equation is unresolved as yet since it requires perfect knowledge of the vertical distribution of the thermospheric heat source.

Evidence favoring a gradient of temperature associated with thermal conductivity in the upper thermosphere is indicated by the occurrence of pronounced diurnal variations of the density. The exact time variations cannot be obtained from a theoretical analysis since the transformation into heat of all ultraviolet radiations is not accomplished instantaneously.

If the diminution of the temperature gradient with height is given by a law of the form

$$\frac{dT}{dr} \propto \Sigma E_{uv}(1 - e^{-\tau}) \tag{35}$$

for an overhead sun, it is not possible to obtain a clear picture of the variation of the heating effect with solar zenith distance. In other words, the relaxation times controlling the thermobalance with internal heat sources cannot be determined since ionospheric reactions are involved.

7. Composition

In the diffusion region the application of Equation 20 can be applied to all constituents (except hydrogen) in the following form

$$\frac{d\rho_i g}{\rho_i g} = -\frac{1 + \beta_i}{\beta_i}\frac{dH_i}{H_i} \tag{36}$$

where

$$H_i = kT/m_i g \tag{37}$$

For a height range in which β is practically constant, Equation 36 is, after integration,

$$\frac{\rho_i g}{\rho_0 g_0} = \exp\left\{-\frac{(1 + \beta_i)z}{\frac{1}{2}(H_i + H_{0i})}\left[1 + \frac{1}{3}\left(\frac{H_i - H_{0i}}{H_i + H_{0i}}\right)^2 + \cdots\right]\right\} \tag{38}$$

and the total density in the heterosphere is determinable when the vertical distribution of each constituent is known. The boundary conditions must be established at a height where diffusion equilibrium conditions are acceptable. In any case, the mean molecular mass, which is fixed by the expression

$$m = \Sigma\rho_i/\Sigma n_i \tag{39}$$

is determined by the boundary conditions.

It is not possible to describe all the atmospheric models which have been proposed. The background of the problem of standard atmospheres can be found in the introduction of *The ARDC Model Atmosphere* by Minzner and Ripley [30], published before the IGY. It will not be discussed here. Before the availability of knowledge resulting from rocket-borne experiments, several attempts were made to extend the standard atmospheres (applied to the homosphere) into the heterosphere. But important modifications were introduced in order to follow the vertical density distribution deduced from the rate of change of the orbital periods of satellites. A first adjustment was made in 1959 to the ARDC atmosphere by Minzner, Champion, and Pond [31]. This led to an increase of ap-

proximately 20 in the density at 600 km. However, the mean molecular mass, about 27.1 at 180 km and decreasing to 17 at 700 km, required a continuous increase of the temperature gradient from 300 km up to 700 km — a gradient rapidly destroyed by conduction in this region.

The Russian model published by Mikhnevich *et al.* [29] corresponded to a temperature gradient only 1°K/km at 250 km and about 7°K/km at 700 km. This is an unacceptable increase of the gradient since it requires a downward heat flow by conduction which is several times greater at 700–500 km than at 250–200 km.

The *COSPAR International Reference Atmosphere* (CIRA) [25] includes references to various proposals made in 1961. It is a matter of fact that there is a tendency among the various authors to adopt isothermal conditions above a certain height, as done by Nicolet [34] who used the same density data deduced from satellite observations as the other workers, contrary to his first proposal [33] of an increasing temperature in the entire heterosphere. In the COSPAR reference atmosphere mean molecular masses are arbitrarily assigned and it is impossible to deduce consistent data for the concentrations. The only parameter deduced from satellite observations (density) does not allow a determination of the

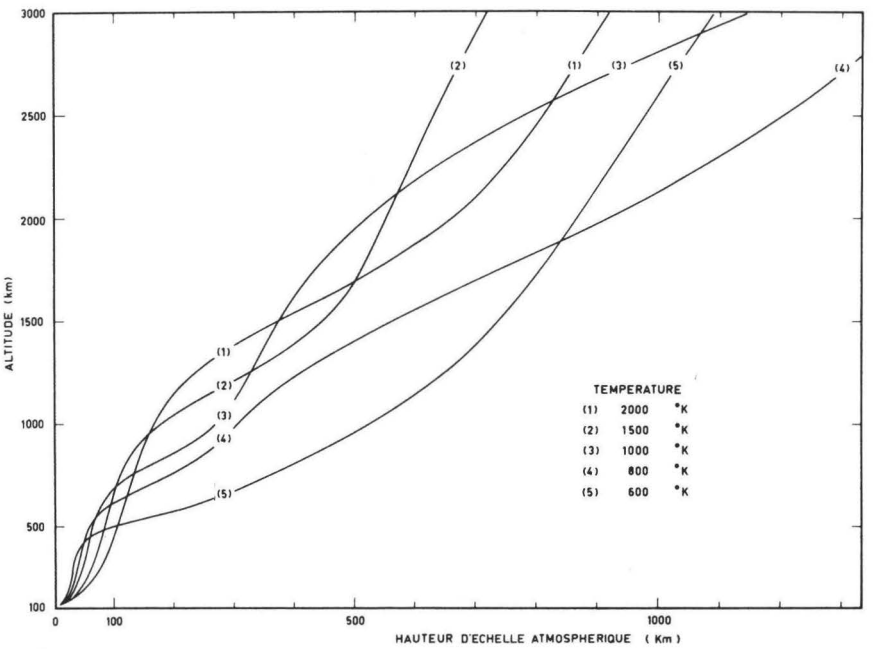

FIG. 10. The atmospheric scale height from 100–3000 km for thermopause temperatures between 600–2000°K. Above 500 km, the variations of the mean molecular mass affect the vertical distribution of the scale height. From Kockarts, to be published in *Bull. Acad. Sciences, Belgium* [26].

composition. Rocket measurements such as those made by the Naval Research Laboratory [9] before the IGY give information about the vertical distribution of molecular oxygen in the thermosphere. More recent measurements using different methods, by Pokhunkov [46], Hinteregger [14], Schaefer and Nichols [50], Jursa *et al.* [23] show that it is still not possible to determine diurnal and/or geographical variations of the density. Factors such as experimental error are too large as yet.

The composition of the heterosphere is certainly affected by varying solar conditions, and boundary conditions cannot be kept constant for a whole solar cycle. For example, if we consider various gradients of the scale height at 150 km with constant boundary conditions at 120 km, i.e., constant density and constant pressure, the density varies by a factor of

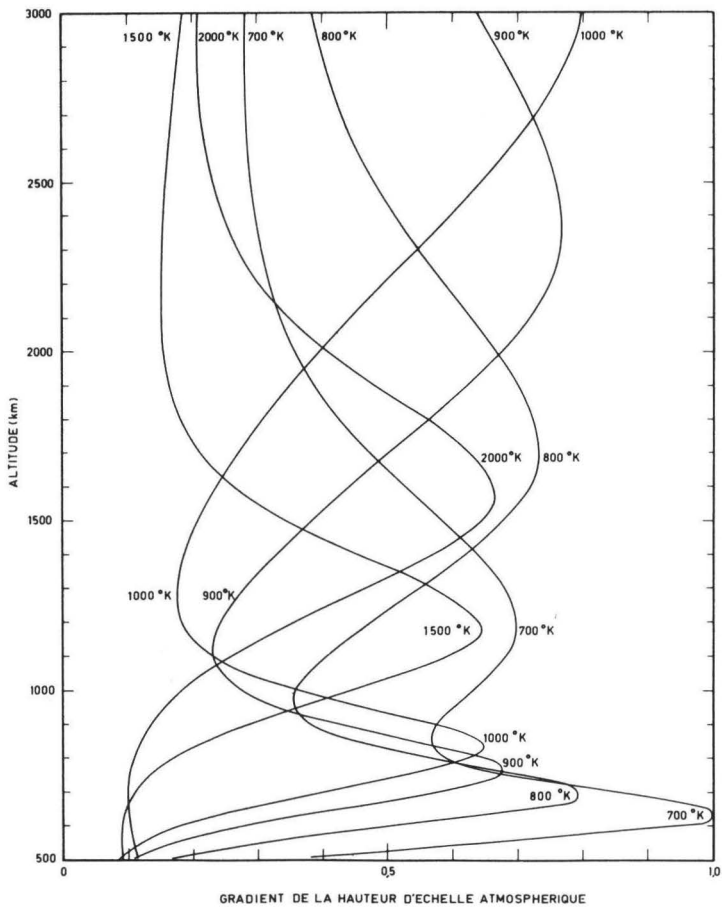

FIG. 11. The scale height gradient from 500–3000 km. Very large variations occur which are often greater than in the thermosphere. From Kockarts, to be published in *Bull. Acad. Sciences, Belgium* [26].

at least 2 at 200 km during a solar cycle. With $\rho = 3.5 \times 10^{-11}$ gm/cm^3 and $p = 2.6 \times 10^{-5}$ mm Hg at 120 km, β varying from $\beta = 0.3$ to $\beta = 0.7$ at 150 km, the density ρ at 200 km is $(3.5 \pm 1.0) \times 10^{-13}$ gm/cm^3. The same density at 200 km can be obtained by assuming a pressure variation of only ± 10 per cent at 120 km and by changing the gradient β by ± 0.1. In other words, atmospheric models must be adapted to the proper solar and atmospheric conditions by a specific temperature gradient in the thermosphere (near 150 km, for example) and by varying boundary conditions at 120 km (for example, by a pressure variation).

As an example of the atmospheric complexity of a complete solar cycle, a general picture of the vertical distribution of the atmospheric scale

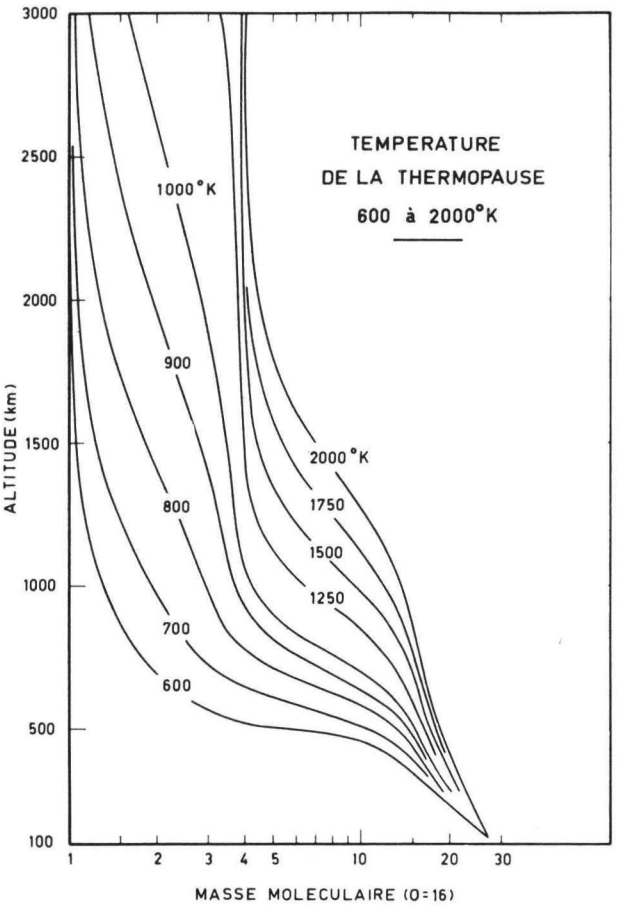

FIG. 12. The vertical distribution of the mean molecular mass from 100 km to 3000 km. For $T \geq 1250$°K, the minimum mean molecular mass, M, is 4, due to helium. For $T \leq 1000$°K, $M < 4$ above 1000 km due to atomic hydrogen. From Kockarts, to be published in *Bull. Acad. Sciences, Belgium* [26].

height and its gradient is given [26] in Figure 10 and 11 for constant lower boundary conditions. The associated variation of the mean molecular mass is shown in Figure 12. The corresponding distribution of N_2, O, He, and H is shown in Figure 13 where the successive belts of atomic oxygen, helium, and atomic hydrogen are indicated by their variation with temperature. Above a certain level, only helium and atomic hydrogen must be

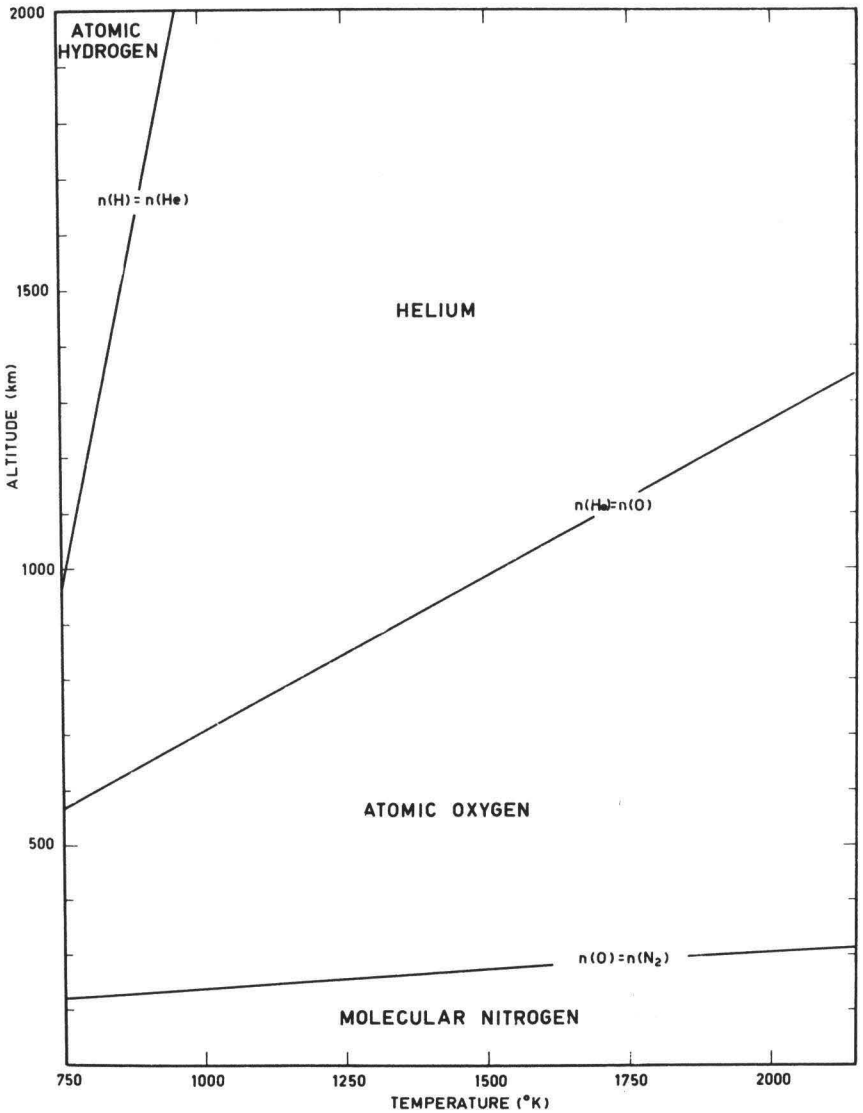

FIG. 13. Distribution of atomic oxygen, helium, and hydrogen belts for thermopause temperatures between 2000–750°K. From Kockarts and Nicolet [28].

considered and a helium-hydrogen atmosphere is subject to special conditions in the exosphere.

This elementary examination of the composition problem of the heterosphere justifies new observational programs for obtaining physical data which cannot be deduced from the analysis of satellite data. The fundamental processes of ultraviolet heating and conductive cooling indicate that atmospheric models for which thermopause temperatures vary between 1000–2000°K are adaptable to daytime conditions. Account must also be taken of the variation of the boundary conditions in order to explain oscillations in the density above the thermopause.

8. Exosphere

Application of Equation 20 above the thermopause leads to

$$\frac{\rho_1}{\rho_{1,a}} = \exp\left[-\left(\frac{a}{r}\right)\frac{r-a}{H_{1a}}\right] \tag{36}$$

where a is the radius at the bottom of the isothermal layer. For a rotating atmosphere, Equation 36 is modified to take into account the effect of the centrifugal force:

$$\frac{\rho_1}{\rho_{1,a}} = \exp\left\{-\left(\frac{a}{r}\right)\frac{r-a}{H_{1,a}}\left[1 - \frac{\omega_e^2}{2ag_a}(r+a)r\sin^2\theta_e\right]\right\} \tag{37}$$

where ω_e is the angular velocity of the earth and θ_e represents the colatitude.

Equation 36 leads to a constant density at $r = \infty$, and Equation 37 to a minimum at about 6.6 earth's radii at the equator. The application of 37 is not generally required since the effect of the centrifugal force is unimportant at the bottom of the exosphere (less than 1 per cent at 1000 km). In any case, the application of 36 and 37 is based on the fact that the velocity distribution is a Maxwellian distribution. In the exosphere the density of a neutral constituent must be defined by a gravitational treatment in which contributions to the density come from various different orbits of particles not subject to collisions. This problem has been studied in detail by numerous authors [1, 7, 8, 11, 13, 21, 22, 41]. It is based largely on the distribution of velocities derived from Liouville's or Boltzmann's equation.

At some height in the exosphere the following components can be introduced, in order to cover all possibilities:

a. Particles related to the critical level:
   1. An elliptic entry component corresponding to particles leaving the critical level with less than the escape velocity.
   2. An elliptic reentry component corresponding to particles returning

to the critical level. In a steady state both components are equal and their density $\rho_1 + \rho_2$ represents a certain fraction ρ_I of the total density at the critical level.

3. A hyperbolic escape component consisting of particles with velocities greater than the escape velocity.
4. A hyperbolic incoming component representing particles arriving at the critical level from the interplanetary space. In a steady state where $\rho_3 = \rho_4$ the total density $\rho_{III} = \rho_3 + \rho_4$ would complete the velocity distribution of particles related to the critical level.

b. Particles not reaching the critical level:

5. An elliptic trapped component corresponding to particles in orbits with perigee above the critical level.
6. A hyperbolic component due to particles not in trapped orbits which should be interplanetary particles.

These last two types of particles, fraction ρ_{II} and ρ_{IV} for elliptic and hyperbolic components, respectively, would complete the distribution of particles at any level in the exosphere, i.e.,

$$\rho_I + \rho_{III} + \rho_{II} + \rho_{IV} = 1 \tag{38}$$

In order to illustrate the dependence of the exospheric components ρ_I, ρ_{III}, ρ_{II}, and ρ_{IV} upon the atmospheric parameters at the critical level, we consider the radius a in Equation 36 as representing the critical level, and we write Equation 36

$$\rho(y) = \rho(1)e^{-E(1-y)} \tag{39}$$

with the following notations used by Öpik and Singer [41]

$$y \equiv a/r \tag{40}$$

leading to $y = 1$ at the critical level and to $y = 0$ at $r = \infty$, and

$$E = a/H_a \tag{41}$$

Assuming a Maxwellian distribution, Equation 39 represents the total density while 38 is the normalization at each altitude of 39: $\rho(y) = 1$. Particles not reaching the critical level are represented by

$$\rho_{II} + \rho_{IV} = (1 - y^2)^{1/2}e^{-Ey^2/(1+y)} \tag{42}$$

and, of course, the particles related to the critical level

$$\rho_I + \rho_{III} = 1 - (1 - y^2)^{1/2}e^{-Ey^2/(1+y)} \tag{43}$$

Under the same conditions, elliptic components are expressed by

$$\rho_I + \rho_{II} = \Phi(Y) + \tfrac{1}{2}\Phi''(Y) \tag{44}$$

where $\Phi(Y) \equiv \Phi[(Ey)^{1/2}]$ is the error function and $\Phi''(Y)$ its second

derivative. Hyperbolic components are expressed by

$$\rho_{III} + \rho_{IV} = 1 - \Phi(Y) - \tfrac{1}{2}\Phi''(Y) \tag{45}$$

Furthermore, the elliptic trapped component ρ_{II} is written

$$\rho_{II} = (1 - y^2)^{1/2} e^{-Ey^2/(1+y)}[\Phi(Z) + \tfrac{1}{2}\Phi''(Z)] \tag{46}$$

where

$$\Phi(Z) \equiv \Phi\left[\left(\frac{Ey}{1+y}\right)^{1/2}\right], \tag{47}$$

while

$$\rho_{IV} = (1 - y^2)^{1/2} e^{-Ey^2/(1+y)}[1 - \Phi(Z) - \tfrac{1}{2}\Phi''(Z)] \tag{48}$$

Equations 42 to 48 indicate that the components at the critical level are expressed by

$$\rho_I = \Phi(E^{1/2}) + \tfrac{1}{2}\Phi''(E^{1/2}) \tag{49}$$

$$\rho_{III} = 1 - \Phi(E^{1/2}) - \tfrac{1}{2}\Phi''(E^{1/2}) \tag{50}$$

$$\rho_{II} = \rho_{IV} = 0 \tag{51}$$

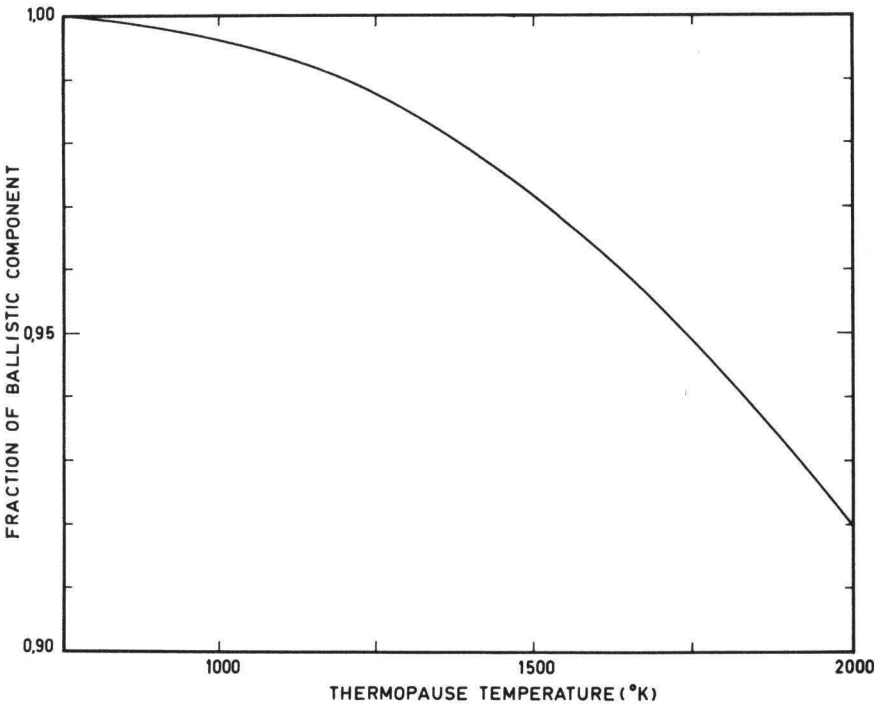

FIG. 14. Density relation of the ballistic component of atomic hydrogen at the beginning of the exosphere, assuming a Maxwellian distribution for the total density $\rho = 1$.

Equations 49 and 50 show that ρ_{III} is practically negligible for a constituent whose escape rate is very small. For example, $\rho_I = 0.9996$ for atomic hydrogen with a thermopause temperature of 750°K or for He^4 with $T = 3000$°K. In other words, the escape component does not play a practical role for helium and heavier atoms in the terrestrial atmosphere. For atomic hydrogen, the effect is not negligible when the temperature

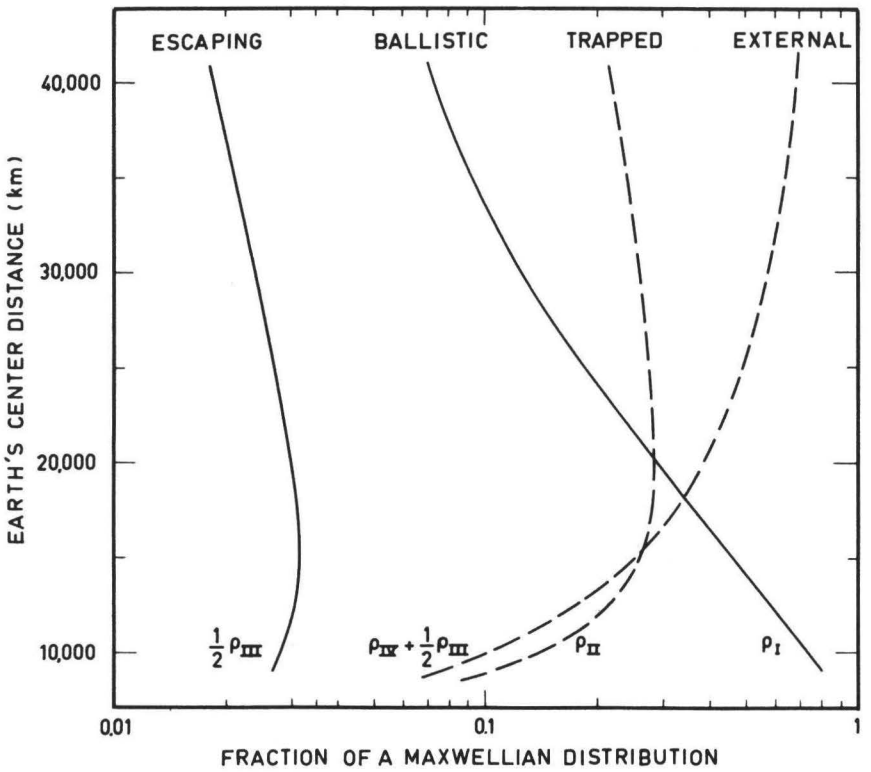

FIG. 15. Exospheric distribution of various components (real and fictitious) of atomic hydrogen for a thermopause temperature $T = 1700$°K. The maximum possible departure from the hydrostatic distribution is shown by trapped and external components. Calculations made in using Godart's formulas [11] and a critical level at 7000 km from the earth's center.

increases. Figure 14 represents the variations of ρ_I (ballistic component) at the critical level between 750°K and 2000°K. The escape component for atomic hydrogen corresponds to about 2.5 per cent at 1700°K and reaches 5 per cent at about 2100°K. This corresponds to the concept of a sharp critical level with no departure from a Maxwellian distribution. Nevertheless, such a concept cannot be accepted since ρ_{III} involves a hyperbolic incoming component which is equal to the escape component.

A Maxwellian distribution therefore cannot be considered as representing real conditions at the critical level. It is useful only as an approximation for determining the escape flux. At $T = 1700°K$, the effusion velocity v_E for a Maxwellian distribution, which is

$$v_E \propto \left(\frac{E+1}{E^{1/2}}\right)e^{-E} \tag{52}$$

leads to

$$v_E(\mathrm{H}) \propto 2.5e^{-4} \tag{52a}$$

$$v_E(\mathrm{He}^4) \propto 4.25e^{-16} \tag{52b}$$

$$v_E(\mathrm{O}) \propto 8.25e^{-64} \tag{52c}$$

for atomic hydrogen, helium, and oxygen, respectively. The approximation is satisfactory when the rate of escape (helium, oxygen) is small but not for atomic hydrogen for which the departure from a Maxwellian distribu-

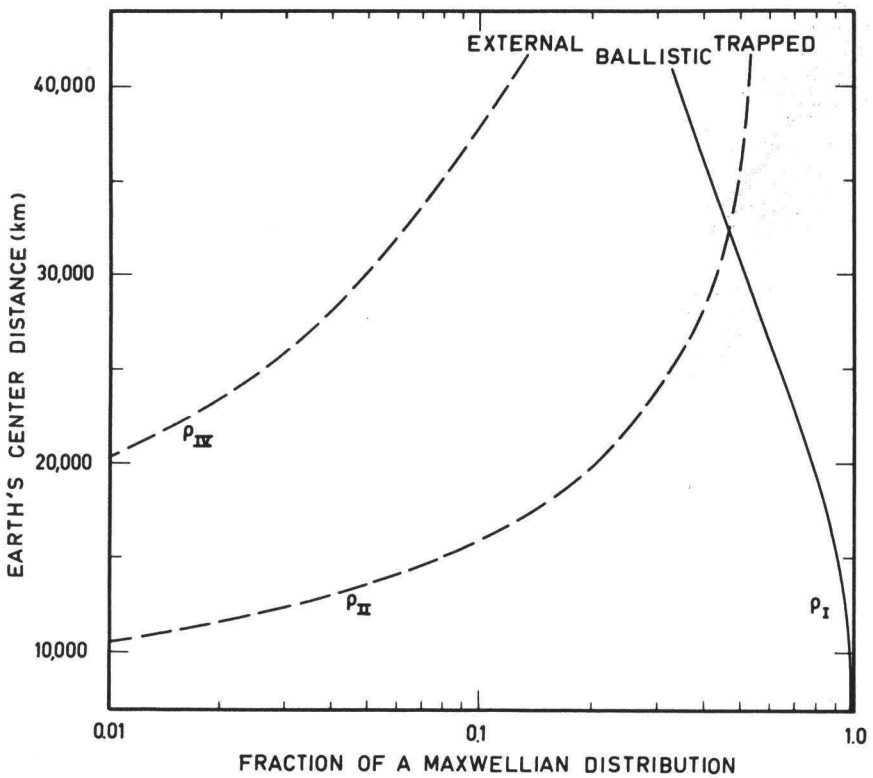

FIG. 16. Exospheric distribution of various components of helium for a thermopause temperature $T = 1700°K$. The ballistic component is relatively more important for helium than for atomic hydrogen.

tion must be introduced in the calculations of the escape flux. There is another aspect which cannot be forgotten for atomic hydrogen: the escape flux is related to the diffusion flux at the bottom of the thermosphere, and the density of atomic hydrogen at the critical level depends on the thermospheric conditions.

It is strictly assumed that there are no collisions in the exosphere; then $\rho_{II} = 0$, i.e., there are no particles in trapped orbits. If no particles are coming from the interplanetary space, $\rho_{IV} = 0$. Under such conditions, Equation 42 would give the fraction of particles which does not enter into

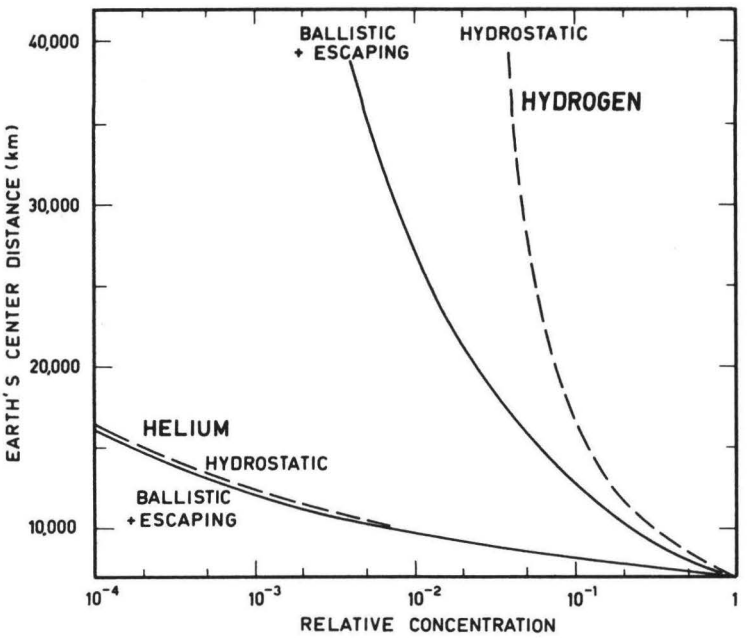

FIG. 17. Relative concentrations of atomic helium and atomic hydrogen in the exosphere at $T = 1700°K$. The hydrostatic distribution and the minimum real distribution are compared.

the hydrostatic equation 39. At $r = \infty$, $\rho_{IV} = 1$, i.e., the total density. Numerical results illustrate (Figs. 15 and 16) the height distribution of the various components in the exosphere for H and He at a thermopause temperature $T = 1700°K$. The escaping component $\frac{1}{2}\rho_{III}$ cannot be neglected for atomic hydrogen but is not important for helium. Figure 17 represents a comparison in the exosphere between the hydrostatic conditions and the minimum density represented by the ballistic and escaping component. Finally, Figure 18 shows the actual distribution when the absolute values of atomic hydrogen and helium concentrations are taken at the critical level. Note that a large variation occurs when the thermo-

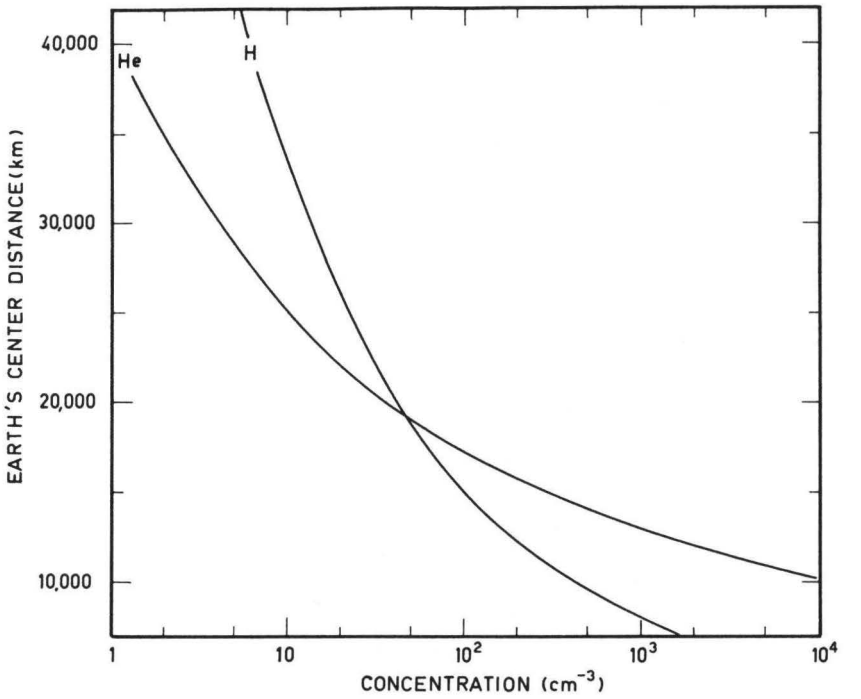

FIG. 18. Absolute concentrations of atomic hydrogen and helium in the exosphere when a Maxwellian distribution is assumed at a critical level corresponding to a distance of 7000 km from the earth's center. There is an identical concentration near 20,000 km for a thermopause temperature of 1700°K.

pause temperature varies since the ratio $n(\mathrm{H})/n(\mathrm{He})$ increases rapidly with decreasing temperature.

The preceding analysis corresponds to an idealization of the exosphere problem. Several physical aspects must be introduced such as the photoionization, and charge exchange processes. In fact, the interaction of the ionized atmosphere with the neutral atmosphere, in addition to the behavior of the superthermal particles, must be considered for the analysis of the transition from the planetary to interplanetary hydrogen [45].

REFERENCES

1. R. E. AAMODT AND K. M. CASE, Density in a simple model of the exosphere, *Phys. Fluids*, **5**, 1019 (1962).
2. D. R. BATES, The physics of the upper atmosphere, *The Earth as a Planet*, G. Kuiper (ed.), Chap. 12 (Chicago Univ. Press, 1954).
3. D. R. BATES AND M. NICOLET, The photochemistry of atmospheric water vapor, *J. Geophys. Res.*, **55**, 301 (1950).
4. D. R. BATES AND T. N. L. PATTERSON, Hydrogen atoms and ions in the thermosphere, *Planet. Space Sci.*, **9**, 959 (1962).

5. L. V. Berkner, G. Reid, J. Hanessian, Jr., and L. Cormier, eds., *Manual on Rockets and Satellites, Annals of IGY, VI* (1958).
6. R. L. F. Boyd and M. J. Seaton, eds., *Rocket Exploration of the Upper Atmosphere* (Pergamon Press, 1954).
7. J. C. Brandt and J. W. Chamberlain, Density of neutral gas in a planetary exosphere, *Phys. Fluids*, **3**, 485 (1960).
8. J. W. Chamberlain, Planetary coronae and atmospheric evaporation, *Planet. Space Sci.*, **11**, 901 (1963).
9. H. Friedman, The sun's ionizing radiations, *Physics of the Upper Atmosphere*, J. A. Ratcliffe (ed.), Chap. 4 (Academic Press, 1960).
10. H. Friedman, Solar radiation, *Astronautics*, **7**(8), 14 (1962).
11. M. Godart, Density of neutral gas in the exosphere, unpublished.
12. I. Harris and W. Priester, Heating of the upper atmosphere, *Space Research III*, 53 (North-Holland Publishing Co., 1963).
13. J. Herring and L. Kyle, Density in a planetary exosphere, *J. Geophys. Res.*, **66**, 1980 (1961).
14. H. E. Hinteregger, Absorption spectrometric analysis of the upper atmosphere in the EUV region, *J. Atmos. Sci.*, **19**, 351 (1962).
15. L. G. Jacchia, Corpuscular radiation and the acceleration of artificial satellites, *Nature*, **183**, 1662 (1959).
16. L. G. Jacchia, Two atmospheric effects in the orbital acceleration of artificial satellites, *Nature*, **183**, 526 (1959).
17. L. G. Jacchia, A working model for the upper atmosphere, *Nature*, **192**, 1147 (1961).
18. L. G. Jacchia, Solar effects on the acceleration of artificial satellites, Smith. Astrophys. Obs., Special Report 29 in Smithsonian Contributions to Astrophysics, **6**, Research in Space Science, Washington, D.C., (1963).
19. L. G. Jacchia and J. Slowey, Accurate drag determinations for eight artificial satellites atmospheric densities and temperatures, Smith. Astrophys. Obs., Special Report 100, Research in Space Science (1962).
20. F. S. Johnson, Temperature distribution of the ionosphere under control of thermal conductivity, *J. Geophys. Res.*, **61**, 71 (1956).
21. F. S. Johnson, The distribution of hydrogen in the telluric hydrogen corona, *Astrophys. J.*, **133**, 701 (1961).
22. F. S. Johnson and R. A. Fish, The telluric hydrogen corona, *Astrophys. J.*, **131**, 502 (1960).
23. A. S. Jursa, N. Nakamura, and Y. Tanaka, Molecular oxygen distribution in the upper atmosphere, *J. Geophys. Res.*, **68**, 6145 (1963).
24. H. Kallmann-Bijl, ed., *Space Research I*, (North-Holland Publishing Co., 1960).
25. H. Kallmann-Bijl, ed., *COSPAR International Reference Atmosphere* (CIRA) (North-Holland Publishing Co., 1961).
26. G. Kockarts, Le problème des hauteurs d'échelle et leurs gradients dans l'hétérosphère, *Bull. Acad. Roy. Sci. Belgique* (1963).
27. G. Kockarts and M. Nicolet, Le problème aéronomique de l'hélium et de l'hydrogène neutre, *Ann. Géophys.* **18**, 269 (1963).
28. G. Kockarts and M. Nicolet, L'hélium et l'hydrogène atomique au cours d'un minimum d'activité solaire, *Ann. Géophys.*, **19**, 370 (1963).
29. V. V. Mikhnevich, B. S. Danilin, A. I. Repnev, and A. V. Sokolov, Certain results in the determination of structural parameters of the atmosphere with the aid of the third Soviet artificial earth satellite, *Iskusstvennye Sputniki Zemli*, **3**, 84 (1959).
30. R. A. Minzner and W. S. Ripley, The ARDC model atmosphere 1956, *Air Force Surveys in Geophysics*, No. 86 (1956).
31. R. A. Minzner, K. S. W. Champion, and H. L. Pond, The ARDC model atmosphere 1959, *Air Force Surveys in Geophysics*, No. 115 (1959).
32. H. E. Newell and L. Cormier, eds., *First Results of IGY Rocket and Satellite Research, Moscow, August 1958*, Annals of IGY, *XII* (1961).
33. M. Nicolet, High atmosphere densities, *Science*, **127**, 1317 (1958).

34. M. Nicolet, Les variations de la densité et du transport de la chaleur par conduction dans l'atmosphère supérieure, *Space Research I*, 46 (North-Holland Publishing Co., 1960).
35. M. Nicolet, Helium, an important constituent in the lower exosphere, *J. Geophys. Res.*, **66**, 2263 (1961).
36. M. Nicolet, Les modèles atmosphériques et l'hélium, *Space Research II*, 896 (North-Holland Publishing Co., 1961).
37. M. Nicolet, Structure of the thermosphere, *Planet. Space Sci.*, **5**, 1 (1961).
38. M. Nicolet, Solar radio flux and temperature of the upper atmosphere, *J. Geophys. Res.*, **68**, 6121 (1963).
39. M. Nicolet, Density of the heterosphere related to temperature, Smithsonian Contributions to Astrophysics, Research in Space Science, **6**, 175 (1963).
40. M. Nicolet, Dynamic effects in the high atmosphere, *The Earth as a Planet*, G. Kuiper (ed.) Chap. 13 (Univ. Chicago Press, 1954).
41. E. J. Öpik and S. F. Singer, Distribution of density in a planetary exosphere, *Phys. Fluids*, **2**, 653 (1959); **3**, 486 (1960); **4**, 221 (1961).
42. D. M. Packer, Altitudes of the night airglow radiations, *Ann. Geophys.*, **17**, 67 (1961).
43. H. K. Paetzold, Solar activity in the upper atmosphere deduced from satellite observations, *Space Research III*, 28, (North-Holland Publishing Co., 1963).
44. H. K. Paetzold and H. Zschörner, The structure of the upper atmosphere and its variations after satellite observations, *Space Research II*, 959, (North-Holland Publishing Co., 1961).
45. T. N. L. Patterson, F. S. Johnson, and W. B. Hanson, The distribution of interplanetary hydrogen, *Planet. Space Sci.*, **11**, 767 (1963).
46. A. A. Pokhunkov, Studies by means of mass spectrometer of parameters of the earth's atmosphere between 100 km and 200 km, *Iskusstvennye Sputniki Zemli*, **7**, 89 (1961).
47. W. Priester, ed., *Space Research III* (North-Holland Publishing Co., 1963).
48. W. Priester, Sonnenaktivität and Abbremsung der Erdsatelliten, *Naturwissenschaften*, **46**, 197 (1959).
49. W. Priester and H. A. Martin, Temperature inversion in the F_1-layer, *Nature*, **188**, 200 (1960).
50. E. J. Schaefer and M. H. Nichols, Neutral composition obtained from a rocket-borne mass spectrometer, *Space Research IV*, 205 (North-Holland Publishing Co., 1964).
51. L. Spitzer, Jr., The terrestrial atmosphere above 300 km, *The Atmospheres of the Earth and Planets*, 213, G. P. Kuiper (ed.) (Chicago Univ. Press, 1949).
52. H. C. van de Hulst, C. de Jager, and A. F. Moore, eds., *Space Research II* (North-Holland Publishing Co., 1961).